

Crawling and Jumping by a Deformable Robot

Yuuta Sugiyama and Shinichi Hirai

Dept. Robotics, Ritsumeikan Univ.
Kusatsu, Shiga 525-8577, Japan
hirai@se.ritsumeai.ac.jp
<http://www.ritsumeai.ac.jp/se/~hirai/>

Abstract. We describe crawling and jumping by a deformable robot. Locomotion over rough terrain has been achieved mainly by rigid body systems including crawlers and leg mechanisms. This paper presents an alternative method of moving over rough terrain, one that employs deformation. First, we describe the principle of crawling and jumping as performed through deformation of a robot body. Second, in a physical simulation, we investigate the feasibility of the approach. Next, we show experimentally that a prototype of a circular soft robot can crawl and jump.

Keywords deformation, locomotion, crawl, jump

1 Introduction and State-of-the-Art

Rough terrain locomotion has mainly relied on rigid body systems, such as crawlers and leg mechanisms. This paper presents an alternative approach that uses deformation.

Recent researches on soft actuators such as shape memory alloy (SMA) wires and polymer gel actuators has yielded impressive results [1–3], and soft actuators have been used to drive leg mechanisms and soft body robots [4]. Unfortunately, soft actuators still have drawbacks. They tend to generate a small force, and those that generate a large force need either a high driving voltage over 1,000V, making it difficult to build self-supporting robots, or a wet environment. To overcome this problem, we employ soft actuators to controllably deform a robot body, enabling it to crawl over and jump on rough terrain. Crawling and jumping using deformation can cope with rougher terrain than rigid body systems can. Additionally, soft body deformation reduces the damage in collision with humans.

In this paper, we propose a circular soft robot and describe its performance in a simulation and in a practical experiment. First, we describe the principle of crawling and jumping as performed through deformation of a robot body. Second, in a physical simulation, we investigate the feasibility of the approach. Next, we show experimentally that a prototype of a circular soft robot can crawl and jump.

2 Principle of Crawling and Jumping by Deformation

Suppose a robot is in stable on the ground, as illustrated in Figure 1-(a). Self-deformation of the robot body generates a moment by a gravitational force around

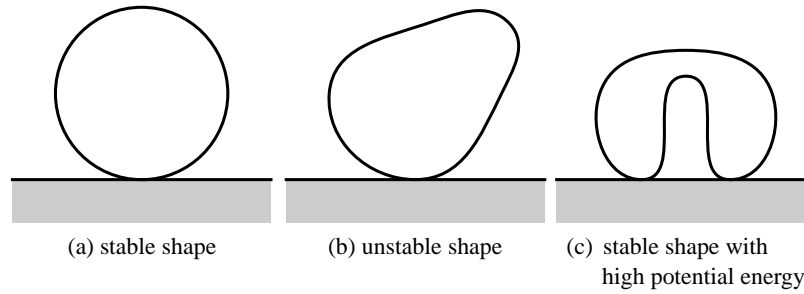


Fig. 1. Principle of crawling and jumping

the area the robot is in contact with the ground. The moment causes the robot to move on the ground. If the robot deforms from a stable shape into an unstable shape described in Figure 1-(b), it rotates clockwise and moves towards the right. Successive deformation of the robot body, which can be generated by actuators, enables a continuous crawling motion along the ground. Thus, the proposed crawling approach uses gravitational potential energy.

Deformation allows elastic potential energy to be stored which, if released rapidly enough, can generate a force large enough to make the robot jump. Now suppose the robot deforms from one stable shape into another, which has large high potential energy as illustrated in Figure 1-(c). If the potential energy is released rapidly enough, the robot will jump. The high-energy shape shown in Figure 1-(c) turns, with a small disturbance, into the stable shape shown in Figure 1-(a), generating the force required for the jump. Thus, the proposed approach uses elastic potential energy. Actuators inside the robot body can be used to store this elastic energy. The forces required to store the elastic energy is generally much smaller than those required to perform a jump.

3 Feasibility Assessment through Physical Simulation

In this section, in a physical simulation, we assess the feasibility of a deformable robot to crawl and jump. As mentioned in the previous section, crawling and jumping can be performed using the elastic potential energy associated with deformation. Let us verify this approach through a physical simulation before we go on to a prototype of a deformable robot.

Let us simulate the behavior of the circular soft robot illustrated in Figure 2. The circular soft robot consists of a circular elastic shell with a set of soft actuators inside, as shown in Figure 2-(a). The robot has eight SMA wires labelled as A through H. Extending or shrinking actuators deforms the robot body, i.e., the circular shell, as shown in Figure 2-(b). We apply open-loop PWM control to the wires. A periodic voltage pattern is applied to the set of SMA wires during crawling. As illustrated in Figure 3, periodic voltage patterns are denoted by the set of wires active during the first time step.

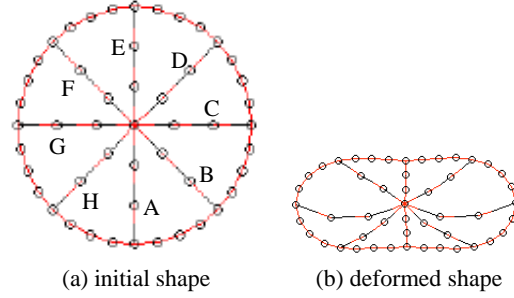


Fig. 2. Circular soft robot

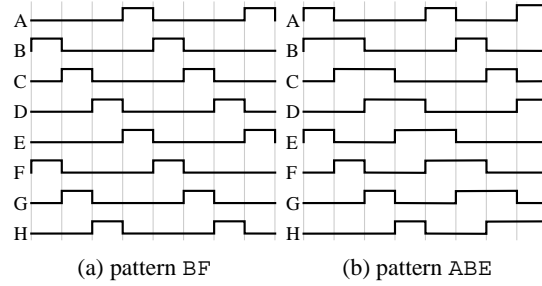


Fig. 3. Voltage patterns applied to SMA wires

The elastic shell of the robot is modeled as an elastic object while actuators are modeled as rheological objects [5], so as to be able to describe the inelastic nature of the SMA wires and polymer gel actuators. We can specify the contraction rate, maximum contraction, and maximum generated force of an SMA wire using a three-element model with a slider.

The extension of an elastic shell is described by a Voigt model, while its bend is modeled as an elastic element. The Voigt model for extension is a parallel connection of an elastic element k_{body} and a viscous element b_{body} . The elastic element for bend deformation is denoted as k_{bend} . We have experimentally identified model parameters for the elastic shell of a prototype of a circular soft robot in advance: $k_{body} = 500\text{N/m}$, $b_{body} = 0.1\text{N/(m/s)}$, and $k_{bend} = 0.0015\text{Nm/rad}$.

Let us first formulate the passive deformation of an SMA wire that deforms in response to an applied external force. SMA wires show both viscoelastic and plastic deformation properties, which suggests their deformation can be modeled by a three-element model. A three-element model is a serial connection of a Voigt element and a viscous element, as illustrated in Figure 4-(a). The elastic coefficient k and damping coefficient b specify the Voigt element, while the viscous coefficient c characterizes the viscous element. Let x be the length of a three-element model. Let x_v and x_d be the lengths of a Voigt model and a viscous element, respectively.

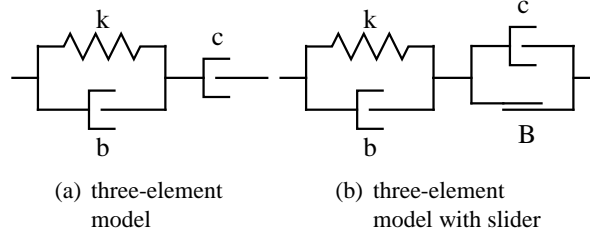


Fig. 4. Model of SMA wires

The three-element model can be formulated as follows:

$$x = x_v + x_d, \quad (1)$$

$$f_{pas} = -kx_v - b\dot{x}_v, \quad (2)$$

$$f_{pas} = -c\dot{x}_d \quad (3)$$

where f_{pas} describes a passive force generated by the element.

A three-element model can extend as long as an external force is applied to it. To avoid such limitless extension, we employ a three-element model with a slider illustrated in Figure 4-(b). The slider is specified by force limit B . In a three-element model with a slider, eq.(3) is replaced by the following equation:

$$-c\dot{x}_d = \begin{cases} f_{pas} & \text{if } fx \leq Bx_v^{\text{init}} \\ 0 & \text{otherwise} \end{cases} \quad (4)$$

where f stands for the resultant external force applied to the element and x_v^{init} is the initial length of the Voigt model in the element.

An SMA wire actively generates a force that is determined by the voltage applied to it. Let us next formulate this actively generated force. Let $V(t)$ be the voltage applied to a wire. We apply open-loop PWM to the generation of a force by a wire. That is, voltage $V(t)$ alternates between V or 0. Let $F(t)$ be a force actively generated by an SMA wire at time t . Let D_{on} be the contraction force rate of the wire and D_{off} its relaxation force rate. Let F_{max} be the maximum force that can be generated by the wire. The force generated by the SMA wire can then be expressed as:

$$\frac{dF}{dt} = \begin{cases} D_{on} & V(t) = V \text{ and } F(t) < F_{max} \\ -D_{off} & V(t) = 0 \text{ and } F(t) > 0 \\ 0 & \text{otherwise} \end{cases} . \quad (5)$$

Integration of the above equation over the time interval $[0, t]$ yields the actively generated force at time t . Note that force $F(t)$ varies in the range $[0, F_{max}]$.

We have used SMA wires BMX100 to build a prototype of a circular soft robot. We have experimentally identified the model parameters to be used in eqs.(1)-(5): $k = 50\text{N/m}$, $b = 0.1\text{N/(m/s)}$, $c = 10\text{N/(m/s)}$, $B = 0.016\text{N}$, $D_{on} = D_{off} = 150\text{mN/s}$, and $F_{max} = 150\text{mN}$.

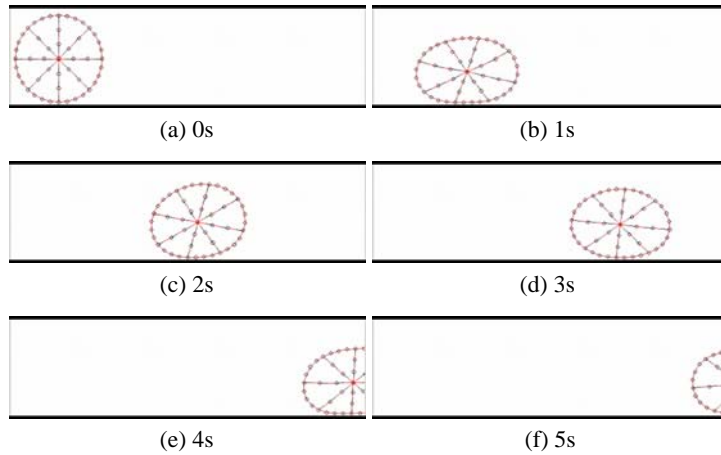


Fig. 5. Simulation of a circular soft robot crawling

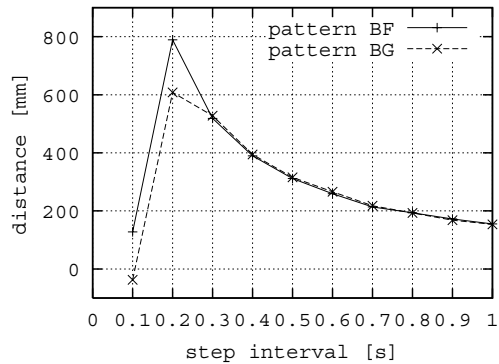


Fig. 6. Comparison of pattern BF and BG

Figure 5 shows the simulation results of the crawling of a circular soft robot. A periodic voltage pattern is applied to one or more of the SMA wires during the crawl. In this simulation, pattern BF illustrated in Figure 3-(a) was used to activate the wires. The figure shows that a circular robot can crawl on a flat terrain by open-loop PWM control of eight SMA wires. Thus, we can find an appropriate voltage pattern through simulation. Figure 6 shows locomotion distances covered over 10s at various step intervals. As shown in the figure, voltage pattern BF with a step interval of 0.2s yields the better result.

Figure 7 shows the simulation results for a jump performed by a circular soft robot. The results suggest that the robot can jump under gravity through PWM control of wires.

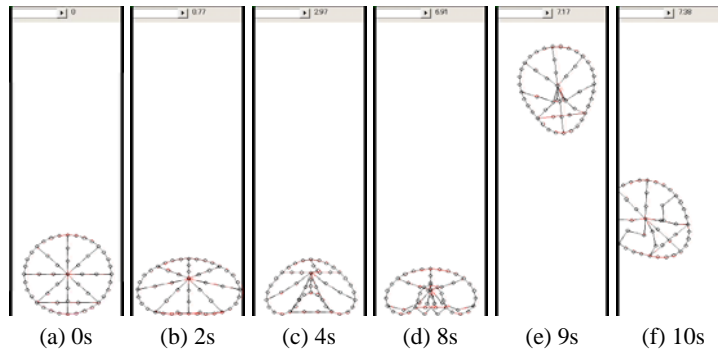


Fig. 7. Simulation of a circular soft robot jumping

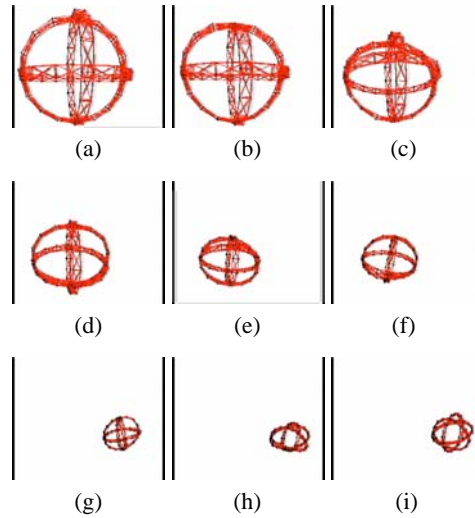


Fig. 8. Crawling of a spherical soft robot

We can simulate the 3D motion of a deformable robot. Figure 8 describes the crawling of a spherical soft robot. The robot consists of three circular elastic shells, which are deformed by contraction of soft actuators located inside the robot.

4 Experimental Results

We build a prototype of a circular soft robot to assess experimentally the feasibility of a deformable robot crawling and jumping. The prototype shown in Figure 9 consists of eight BMX100 SMA wires, labelled A through H, attached to the inside of a circular rubber shell. The diameter of the circular body is 40mm and the robot weighs 3g. When voltage is applied to a wire, it contracts, resulting in the circular

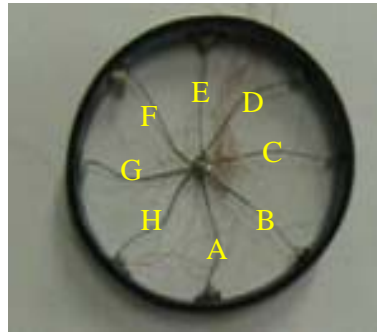


Fig. 9. Prototype of a circular soft robot

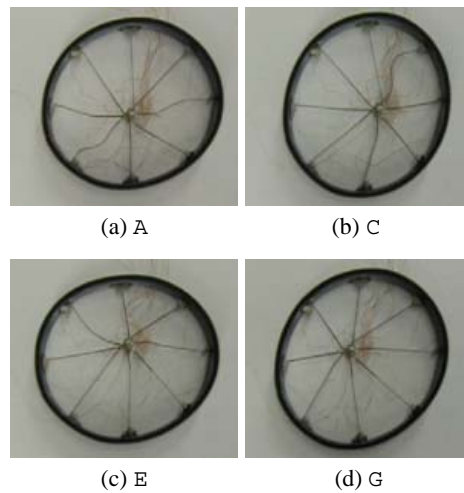


Fig. 10. Deformation of a circular soft robot

rubber deforming as shown in Figure 10. Each figure corresponds to the deformation caused by the contraction of an individual wire.

Figure 11 shows a sequence of snapshots of the prototype crawling. Voltage pattern BF is applied to SMA wires. As shown in the figure, the circular robot can crawl on a flat ground.

Let us compare the simulation and experimental results for crawling. Figure 12 describes locomotion distances covered over 10s at various step intervals. The prototype moves 260mm over 10s at a step interval of 0.6s. As shown in the figure, simulation results agree with experimental results. Reducing the step interval results in faster locomotion.

Figure 13 shows a sequence of snapshots of the prototype climbing a slope. The prototype can climb up a slope of 20° by applying pattern ABE illustrated in Figure 3-(b).

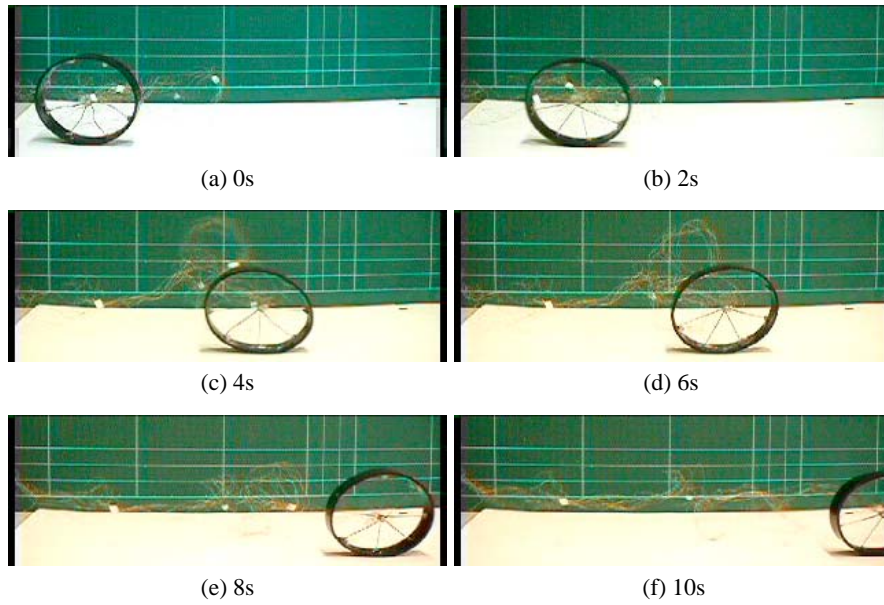


Fig. 11. Circular soft robot crawling

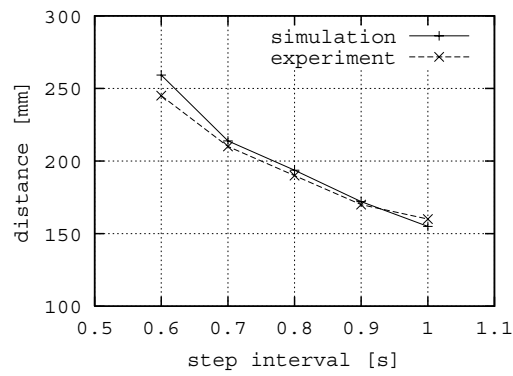


Fig. 12. Comparison between simulation and experimental results for voltage pattern BF

Figure 14 shows a sequence of snapshots of the prototype jumping. The prototype can jump a distance of 80mm, which is twice its diameter.

5 Conclusion and Research Perspective

In the present study, we proposed a deformable robot capable of crawling and jumping. First, we described the principle of crawling and jumping using the deformation of a robot body. Second, in a physical simulation using a three-element model

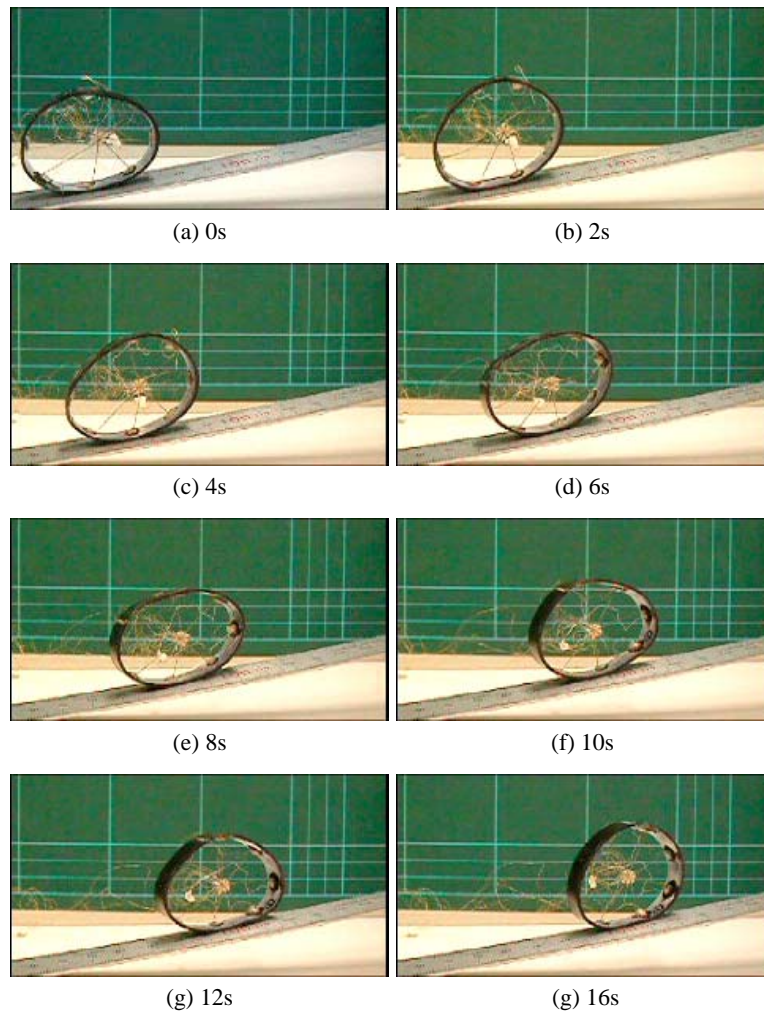


Fig. 13. Circular soft robot climbing a slope

with a slider, we show the feasibility of the robot to crawl and jump. Finally, we experimentally verified that a prototype of a circular soft robot can crawl and jump.

To date, no analysis has been conducted on the motion of a circular soft robot. In further studies, we will apply linear object modeling [6] to analyze and optimize the motion of a circular robot. We will evaluate the potential energy of a circular soft robot during crawling and jumping in order to get a better understanding of the system. We will also make a prototype of a spherical soft robot capable of performing 3D motion.

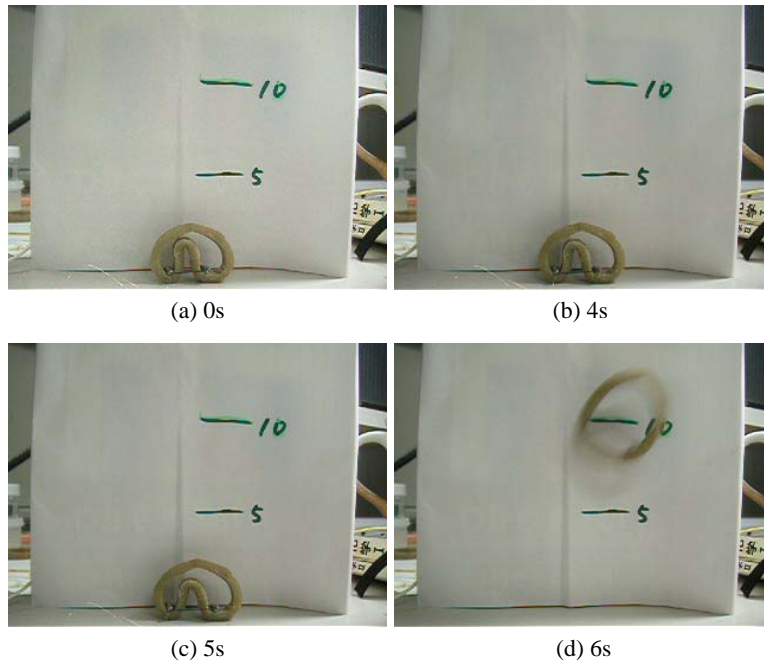


Fig. 14. Circular soft robot jumping

Acknowledgement

This research was supported in part by the Ritsumeikan University 21st Century COE program “Micro Nanoscience Integrated Systems”.

References

1. Pelrine, R., Kornbluh, R., Pei, Q., and Joseph, J., *High-speed Electrically Actuated Elastomers with Strain Greater Than 100%*, *Science*, Vol. 287, February, pp.836–839, 2000.
2. *The First Conference on Artificial Muscles*, December, 2001.
3. *Artificial Muscles*, *Scientific American*, October, pp.34–41, 2003.
4. Otake, M., Kagami, Y., Inaba, M., and Inoue, H., *Motion design of a starfish-shaped gel robots made of electroactive polymer gel*, *Robotics and Autonomous Systems*, Vol. 40, pp.185–191, 2002.
5. Kimura, M., Sugiyama, Y., Tomokuni, S., and Hirai, S., *Constructing Rheologically Deformable Virtual Objects*, *Proc. IEEE Int. Conf. on Robotics and Automation*, Taipei, September, 2003.
6. Wakamatsu, H. and Hirai, S., *Static Modeling of Linear Object Deformation based on Differential Geometry*, *Int. J. Robotics Research*, Vol. 23, No. 3, March, pp.293–311, 2004.